International Journal of Research in Medical and Basic Sciences, ISSN: 2455-2569

Vol.03 Issue-02, (February, 2017), ISSN: 2455-2569, Impact Factor: 4.457

Mass and Energy balance in a greenhouse

Juwawa Chayangira
Department of Physics, Geography and Environmental Science
Great Zimbabwe University
P.O Box 1235 Masvingo, Zimbabwe

Abstract

The main driving force in a greenhouse is ventilation in terms of both the energy and mass constituents. To have a favourable climatic condition both energy and mass balance should be monitored. This study aims to implore this energy and mass balance affect the microclimatic condition in a greenhouse. It was found out the energy balance plays a critical role in plant growth through its effect on transpiration, while the mass balance was found to affect through carbon dioxide penetration and movement of water vapour which can also affect energy balance through the release of latent heat. The water vapour balance method was used to determine the transpiration rates. The energy balance was evaluated using the Penman Monteith method. The green house ventilation rate which plays the pivotal role in the energy and mass balance in a greenhouse was also evaluated.

Mass and Energy balance in the greenhouse

2.2.1 Greenhouse Energy Balance

Ventilation removes energy from a greenhouse and prevents high temperatures during periods of high insolation. For a greenhouse with no heating, the energy removed by the process of leakage and ventilation is equal to the solar collected in the greenhouse minus the thermal losses through the cover minus the energy stored. The energy lost by leakage and ventilation has two components, one component due to sensible heat, and the other component due to latent heat.

For the energy balance of a greenhouse, the energy inputs equal the sum of energy losses and the greenhouse transient energy content, the energy inputs result from the absorption of long and short wave radiation. The net radiometer can be estimated from the net radiometer installed between the top of the crop canopy and the cover. The net radiation is partly absorbed by the protected crop and the other part is transmitted through the crop canopy where it is absorbed by the greenhouse soil surface (Demrati,et al,.2001).

$$R_{net} = R_{a,v} + R_{a,s} \qquad (2.11)$$

Where $R_{a,v}$represents part of radiation absorbed by the vegetation inside the greenhouse.

$R_{a,s}$represents part of net radiation absorbed by the greenhouse soil surface.

Thus this radiation absorbed by the crop and soil surface contributes to the inside air heating resulting from sensible heat from vegetation and soil which are given the following symbols $H_{v,i}$

in Wm^{-2} and $H_{s,i}$in Wm^{-2} and subscript i denotes inside, and the also has the effect of increase of water vapour content through increase of latent energy from the crop and soil $\lambda E_{v,i}$and $\lambda E_{s,i}$and heat the thermal mass of the crop and soil.

The thermal balance of the crop inside the greenhouse is therefore given by the relation below

$$R_{a,v} = H_{v,i} + \lambda E_{v,i} + \rho_v c_v l_v \frac{dT_v}{dt} \qquad (2.12)$$

Where $H_{v,i}$is the sensible flux exchanged between the vegetation and inside air in Wm^{-2}, $\lambda E_{v,i}$ is the latent flux exchanged between the vegetation and inside air in Wm^{-2}, ρ_v is the density of vegetation in kgm^{-3}, c_v is the specific heat in $Jkg^{-1}K^{-1}$, l_v is the mean equivalent height of crop in m, T_v is the temperature of vegetation in ^oC and t is the time in s.

Similarly, the diurnal thermal balance of the soil surface is

$$R_{a,s} = H_{s,i} + \lambda E_{s,i} + F_s + \rho_s c_s l_s \frac{dT_s}{dt} \qquad (2.13)$$

Where $H_{s,i}$is the sensible flux exchanged by convection between the soil and inside air in Wm^{-2}, $\lambda E_{s,i}$is the latent flux exchanged between the soil surface and inside air in Wm^{-2}, ρ_s is the density of soil in kgm^{-3}, l_s is the thickness of the soil layer in m, $c_s$is the specific heat of soil in $Jkg^{-1}K^{-1}$, Ts is the temperature of soil in ^oC and t is the time in s. $F_s$is thethermal flux in the soil in Wm^{-2} (positive when moving from air to the soil)

When neglecting the energy storage terms for long time steps and condensation during daytime and substituting equations (1) and equations (3), equation (1) becomes

$$R_{net} = H_{v,i} + H_{s,i} + \lambda E_{v,i} + \lambda E_{s,i} + F_s \qquad (2.14)$$

The term ($H_{s,i}$+ $H_{v,i}$) represents the greenhouse sensible heat gain which is either evacuated by ventilation flux, or exchanged with the greenhouse roof and side walls. The term ($\lambda E_{v,i}$+ $\lambda E_{s,i}$) represents the greenhouse latent heat gain which is evacuated by ventilation flux, and increases the inside air latent heat content.

2.2.2 Greenhouse Vapour Balance

Evaporation of small droplets of water, evaporation from wet soil or surfaces, and transpiration are all influenced by the vapour content of nearby air. If the air is saturated evaporation will occur, if not evaporation can proceed (Rosenberg, 1983). Evaporation or evapotranspiration increases in response to an increasing difference between the vapour pressure at the evaporating surface and the vapour pressure of air (vapour pressure deficit). The humidity build up in the greenhouse are transferred to the outside by ventilation. The temperature of the air and or that of the evaporating surface exerts a major influence on evapotranspiration. In general the higher the temperature, whether of air or evaporating surface, the greater will the rate of evaporation. Because of the strong dependence of evaporation on temperature and because temperature is good integrator of several environment variables, many models for predicting ET use temperature as a major unit. Temperature influences evapotranspiration in the following four ways. The amount of water vapour that air can hold increases exponentially with increasing temperature. As the surface temperature increases the vapour pressure at the evaporating surface increases as does the vapor pressure between the surface and nearby air. Because air can hold more vapour as its temperature increases the vapour pressure deficit between surface air and the evaporating surface becomes larger and evaporative demand is increased as air is warmed. Warm dry air may supply energy to an evaporating surface. The rate of evaporation is dependent on the amount of heat transferred, therefore the warmer the air the stronger the temperature gradient and the higher rate of evapotranspiration. If it is the evaporating surface that is warmed less, sensible will be extracted and evaporation will decrease.

2.3 Ventilation

The main driving forces of ventilation for a greenhouse with both roof and side vents are:

1. The chimney effect, due to thermal buoyancy forces (Bruce, 1982), aiming at a vertical distribution of pressures between the side and roof openings.
2. The static wind effect due to the mean component of the wind velocity, which induces a spatial distribution of pressures over the envelope of the greenhouse.
3. The turbulent effect of the wind, linked to the pressure fluctuations of the wind velocity along openings (Boulard and Baille, 1995), inducing an influx and out flux within the same opening.

The static wind effect give rise to a vertical distribution of pressures between the side and roof openings (1978) and to a horizontal distribution of pressures between the upwind and the downwind parts of the greenhouse (Hoxey and Maron, 1991; Boulard et al 1991) resulting in “side wall effect” already analyzed by several authors (De Jong, 1991; Fernandez and Bailey, 1992)

Two main air fluxes are generated by these effects:

(a) A vertical ventilation flux due to chimney effect and the vertical static wind pressure distribution.

(b) A horizontal ventilation flux due to side wall effect and the turbulent effect.

2.3.1 Vertical Ventilation Flux

Air flow through an opening is caused by a combination of pressure differences induced by the buoyancy forces (the chimney or the stack effect) and the wind forces.

Considering a greenhouse equipped with roof and side openings. If the wind is parallel to the ridge, then static wind pressure coefficients of the roof openings are identical (C_R), the same is valid for the side openings which are characterized by a common static wind pressure coefficient (C_S) (Baille, 1992: Gandemer and Bietry, 1989).

The vertical air flow exchanged between the side (S) and the roof(R) openings is composed of two parts, thermal buoyancy and wind effect.

$$G_V = C_d \frac{A_R A_S}{\sqrt{A_R{}^2 + A_S{}^2}} \left[2g \frac{\Delta T}{T_0} + (C_R - C_S) u^2 \right]^{0.5} \qquad (2.15)$$

Where G_v = vertical ventilation flow rate (m^3s^{-1}) exchanged between the side and roof openings.

C_d = discharge coefficient

A_R= roof openings area (m^2)

A_S = side openings area (m^2)

g = acceleration due to gravity (ms^{-2})

ΔT = difference between inside and outside temperature (K)

T_o = outside temperature (K)

h = vertical distance between the midpoint of the side and roof openings (m)

C_R = static wind pressure coefficient at the level of roof openings

C_S = static wind pressure coefficient at the level of side openings

u= wind velocity (ms^{-1}) at 4.5 m above the ground

Assuming that C_R-C_S=k equation 1 becomes

$$G_v = C_d \frac{A_R A_S}{\sqrt{A_R{}^2 + A_S{}^2}} \left[2g \frac{\Delta T}{T_o} h + ku^2 \right]^{0.5} \qquad (2.16)$$

2.3.2 Horizontal ventilation flux due to side wall and turbulent effects

A wind parallel to a continuous opening extended along a building gives rise to a static pressure field near the edges of the building, which induces a steady influx at the leeward and an out flux at the windward part (Boulard et al, 1995) This is known as the "side wall" effect and is linked to a pressure gradient along the opening. Its contribution to the total ventilation flux is important and varies inversely to the size of the greenhouse (Fernandez and Bailey, 1992).

Wind turbulence, in interaction with the structure or with immediate surrounding, create fluctuating pressures around the greenhouse, which induce two ways airflow through the same opening (Van der Moas, 1992). In a greenhouse equipped with only roof openings the air flow enters and leaves the building through the same opening so that inflow area is equal to outflow area over time (Bot, 1983; Boulard, 1993). In a case where both roof and side ventilators are open, the ventilation area is considered to be half of the total vents area. The global wind coefficient C_w can be defined as the coefficient which includes both the turbulent and side wall effects and thus horizontal wind driven flux G_h is equal to

$$G_h = \frac{A_T}{2} C_d \sqrt{C_w} u \qquad (2.17)$$

Where

$$\frac{A_R + A_S}{2} = \frac{A_T}{2} \qquad (2.18)$$

G_h = horizontal ventilation flow rate (m^3s^{-1})

A_T= total area of vents (m^2)

C_w= global wind coefficient

This expression of horizontal ventilation flux is similar to that given by several authors (Boulard, 1993; Kittas et al 1995) for greenhouse with only roof vents

Combination of the Vertical and Horizontal Fluxes

We can combine these fluxes through either (Boulard&Baille, 1995)

The algebraic sum:

$$G = G_v + G_h \tag{2.19}$$

Where G is the total ventilation flow rate (m^3s^{-1})

The vertical sum:

$$G = \sqrt{G_v^{\,2} + G_h^{\,2}} \tag{2.20}$$

In this case, the flow is driven by the pressure field equal to the sum of two forces (stack and wind)

Local estimation of air flows and energy fluxes along a continuous roof opening, using eddy correlation techniques (Boulard et al, 1995), has shown that the 'side wall' effect was much greater than the turbulent effect

Hence the static pressure field linked to the wind effect can thus be combined with static pressure field linked to buoyancy forces through a vectorial sum of G_v and G_h

$$G = C_d \left[\left(\frac{A_R A_S}{\sqrt{A_R^{\,2} + A_S^{\,2}}} \right)^2 \left(2g \frac{\Delta T}{T_o} h + ku^2 \right) + \left(\frac{A_T}{2} \right)^2 C_w u^2 \right]^{0.5} \tag{2.21}$$

From studies of Kittas, Papadakis and Boulard it was revealed that the vertical air flow due to wind driven static pressure has the same direction as the airflow which is induced by the chimney effect, however, the k value was found to be small and statistically not significant and it means that wind flux generated by the vertical distribution of pressures is negligible, and a large part of the static wind effect is already explained by C_w neglecting K equation 2.21 becomes

$$G = C_d \left[\left(\frac{A_R A_S}{\sqrt{A_R{}^2 + A_S{}^2}} \right)^2 \left(2g \frac{\Delta T}{T_o} h \right) + \left(\frac{A_T}{2} \right)^2 C_w u^2 \right]^{\circ 0.5}$$

(2.22)

2.4 Methods of determining the ventilation rate

2.4.1 Tracer gas technique

The tracer gas technique is one of the most important techniques for measuring ventilation and leakage rates which has been used by (Bot (1983), Nederhoff et al 1985, De Jong 1990, Fernandez and Bailey (1993) and Boulard et al (1993). The tracer gas technique is based on a mass balance of a tracer gas in the greenhouse air.

There are two main methods of measuring ventilation and leakage rates which are

a) the continuous injection or static method.

b) the pulse injection or dynamic method

The characteristics of the tracer gas are based on the following, easy to measure at low concentrations, inert, non-toxic, non flammable, not a natural component of air and with a molecular weight close to the average weight of the air components. The gases which are used as tracer gases include sulphur hexafluoride (SF_6, methane (CH_4), carbon dioxide (CO_2), hydrogen (H_2), nitrous oxide (N_2O), argon 41 and krypton 85. The most commonly used gases are carbon dioxide and nitrous oxide. Nitrous oxide is the best because it meets all the above requirements, carbon dioxide can be used, but it is necessary to measure the concentration of CO_2 in the external air and rate of release from the soil. In a greenhouse with crops, N_2O is the better of the two because its concentration is not affected by the photosynthesis and respiration of the plants.

2.4.1.1 Static method

In this method, the injection rate of gas into the greenhouse is held at a constant value until an equilibrium concentration is reached. The gas supply and sampling system must be distributed around the greenhouse in order to obtain good dispersion of the gas and uniform sampling of the air. The ventilation rate is calculated from

$$G = \frac{M}{\left[C_{i(t1o)} - C_{0(t1)}\right]} - \frac{V}{t_2 - t_2} \times \ln\left[\frac{C_{i(t2)} - C_{o(t2)}}{C_{i(t1)} - C_{0(t1)}}\right] \qquad (2.23)$$

Where M is the mass flow of gas entering the greenhouse

$C_i$and C_o are the internal and external gas concentration

V is the volume of the greenhouse, and t_1 and t_2 are sequential measurements.

The advantage of this method is that it provides continuous information, and a range of wind speed and direction can be covered during one measurement. The disadvantage is the high consumption of tracer gas.

2.4.1.2 Dynamic method

In this method, the tracer gas is injected and distributed uniformly in the greenhouse until a certain pre-determined concentration is reached and then stopped. The decay in the concentration of the tracer gas is then measured. When the concentration has decreased to 80-90% of the initial value, another pulse of gas is injected, and decay is measured. It is possible to change the angle of ventilator opening on each decay but not during one period of decay.

The ventilation rate is calculated by the following procedure

the natural logarithm of $(C_i\text{-}C_o)$ is plotted against time

A time period t is selected during which ln $(C_i\text{-}C_o)$ decreases linearly.

A linear regression is fitted to the values of ln$(C_i\text{-}C_o)$ over this period

$$\ln (Ci - C_o) = a + Rat \qquad (2.24)$$

Where Ra is the ventilation rate in air changes per hour and a is a constant. The air renewal rate is negative because the concentration of the gas decreases during measurement. The ventilation rate G in m^3/s is given by

$$G = \frac{R_a V}{3600} \qquad \textbf{(2.25)}$$

Mean values are obtained for the wind speed, wind direction and internal and external temperature, over the time period selected.

The advantages of the decay method over the static method are that it uses less tracer gas and can be used to measure over a wide range of ventilation rates while the continuous injection method requires an appropriate flow meter to measure the injection rate. The disadvantages are the difficulty in obtaining a uniform concentration of the tracer gas throughout the greenhouse and for high ventilation rates, the concentration of the gas decreases rapidly and the data obtained for analysis can be insufficient.

2.4.2 The water vapour balance method

Assuming (i) Perfect mixing of water vapour in the volume of the greenhouse, and (ii) that evaporation from the soil and/ or other medium is negligible (justified by the presence of a plastic mulch on the soil surface and the cover offered by the crop); the greenhouse ventilation rate, G can be calculated from mass balance of water vapour of the greenhouse:

$$V\frac{dx_i}{dt} = G(t).\left[x_e(t) - x_i(t)\right] + T_r(t) \qquad (2.25)$$

Where G(t) is the ventilation rate (m^3/s), V is the greenhouse volume (m^3), x_i and x_e are the inside and outside air absolute humidity, respectively (kg/m^3), and T_r (t) is the greenhouse crop transpiration rate (kg/s)

For small time steps, Δt Equation (2) can also be expressed as:

$$V\frac{\Delta x_i}{\Delta t} = V\frac{x_i(t+\frac{\Delta t}{2}) - x_i(t-\frac{\Delta t}{2})}{\Delta t} = G(t).\left[x_e(t) - x_i(t)\right] + T_r(t) \qquad (2.26)$$

So that:

$$G(t) = \frac{\left[V \dfrac{x_i\left(t + \dfrac{\Delta t}{2}\right) - x_i\left(t - \dfrac{\Delta t}{2}\right)}{\Delta t} \right] - T_r(t)}{\left[x_e(t) - x_i(t)\right]}$$

(2.27)

Measured values of air temperature and relative humidity outside and inside the greenhouse (at 30-minute time steps) will be used to calculate the values of outside and inside greenhouse air absolute humidity, respectively. These values and the crop transpiration rate , $T_r(t)$, obtained from measurements of sap flow, leaf area and the leaf area index will then be used to calculate the greenhouse ventilation rate , and hence the air renewal rate, using equation (2.27)

The absolute humidity in equation (2.27) are evaluated from the from relationship as given by Jones (1992)

$$x = \frac{2165}{T} * e \qquad (2.28)$$

Where x is the absolute humidity in kgm^{-3}, T is air temperature and e is the actual vapour pressure (kPa).

The areas of the vent openings will be calculated by using the control algorithm of the ventilation control system and compared to a few values measured on selected days and at selected times of the day.

Leakage rates will be calculated as the average value of the ventilation rates when the greenhouse is closed.

2.5 Determination of Transpiration Rate

The transpiration rate in a greenhouse can be determined by using many methods which include eddy-correlation, aerodynamic techniques, Bowen approaches and combination or energy balance methods. Fuchs (1973) examined these methods and separated them as to energy balance, mass and heat transport, and turbulent mixing, aerodynamic and the Bowen ratio method. The Penman Monteith can be used to evaluate transpiration rate in a greenhouse and it is formulated from the following basic principles.

Penman in 1948 combined the energy balance with mass transfer method and derived an equation to compute the evaporation from an open water surface from standard climatological records of sunshine,

temperature, humidity and wind speed. This is the combination method which was further developed by many researchers and extended to cropped surfaces by introducing resistance factors. The resistances are aerodynamic resistance and surface resistance. The surface resistance, r_s describes the resistance of vapour flow through the stomata openings, total leaf area and soil surface. The aerodynamic resistance, r_a, describes the resistance from vegetation upward and involves friction from air flowing over the vegetative surface.

2.5.1 Penman-Monteith Method for determining transpiration

The Penman-Monteith form of the combination equation is as follows:

$$\lambda E_T = \frac{\Delta(R_n - G) + \rho_a c_p \dfrac{(e_s - e_a)}{r_a}}{\Delta + \gamma\left(1 + \dfrac{r_s}{r_a}\right)} \qquad (2.29)$$

Where R_n is the net radiation, G is the soil heat flux, $(e_s\text{-}e_a)$ represents the vapour pressure deficit of the air, ρ_a is the mean air density at constant pressure, c_p is the specific heat of air, Δ represents the slope of the saturation vapour pressure temperature relationship, γ is the psychometric constant, and r_s and r_a are the (bulk) surface and aerodynamic resistances respectively.

Transpiration in a greenhouse is generally from the understanding that the rate of transpiration depends on the amount of radiative energy absorbed by the canopy, R_A, and on the vapour pressure deficit, $D=e_s(T)\text{-}e$, $e_s(T)$ being the saturated pressure vapour deficit(mb) at temperature T. The transpiration is expressed by means of Penman-Monteith formula (Monteith 1973) extended to the whole canopy considered as a "big leaf".

$$TR = \frac{\Delta}{\Delta + \gamma^*} \bullet \frac{R_A}{\lambda} + \frac{\rho_a c_p}{\lambda} \bullet \frac{r_a D}{\Delta + \gamma^*} \qquad (2.30)$$

Where TR = transpiration rate ($kgm^{-2}s^{-1}$)

R_A =radiation absorbed by the canopy (Wm^{-2})

λ =latent heat of vaporization (Jkg^{-1})

$\rho_a c_p$=volumetric heat capacity of air ($Jm^{-3}\ °C^{-1}$)

$$\gamma^* = \gamma\left(1+\frac{r_a}{r_s}\right)$$ = γ being the psychometric constant, $r_a$and r_s (ms^{-1}) respectively the aerodynamic and stomatal conductance of the canopy to water vapour transfer. The psychometric constant ($kPaK^{-1}$) is depend on pressure and latent heat of vaporization

$$\gamma = \frac{Pc_p}{0.622\lambda} \quad (2.31)$$

and λ in $kJkg^{-1}$ is given by the relationship below, where P is the pressure (kPa)

$$\lambda = 10000(2501 - 2.361T) \quad (2.32)$$

$$P = 101.3\left[\frac{293 - 0.0065E_L}{293}\right]^{5.26} \quad (2.33)$$

Where P is the barometric pressure in kPa, calculated from elevation (E_L) in m above sea level (Jensen, Burman and Allen, 1990)

Δ = slope of the water vapour saturation curve

$$\Delta = \frac{4098e_s}{(T+273.3)^2} \quad (2.34)$$

in ($kPa°c^{-1}$) and $e_s$in kPa and T in °C, the saturation vapour pressure of the air when the number of water molecules condensing equals the number evaporating from a flat surface of water with both the air and water vapour at some temperature, T. An equation for the saturation vapour pressure (e_s) over water at

temperature, T, (^oC) was given by (Tetens, 1930) as

$$e_s = 0.6108\exp\left(\frac{17.27T}{(T+237.3)^2}\right) \quad (2.35)$$

In greenhouse conditions, r_a = 200 sm^{-1} was chosen as a representative value of leaf aerodynamic resistance(Seginer,1984, Stanghellini, 1987; Baille et al , 1994c; Kittas et al ,1999)

2.5.2 Sap flow gauge method of determining transpiration rates

2.5.2.1Stem heat balance basics

The stem heat balance (SHB) requires a steady state and constant energy input from the heater strip inside the gauge body. Therefore the stem section must be insulated from changes in the environment. For the same reason, the gauge time constant is limited from five minutes to an hour, depending on the flow rate and the stem size. The Dynamax loggers have a power down mode so that power is saved at night and the stem is preserved from overheating. During the power down mode and at the transitions to power on, sap flow is not computed to maintain the accumulated flow accurately the measurement.

Figure3.2 shows a stem section and the possible components of heat flux, assuming no heat storage. The heater surrounds the stem under test and is powered by a DC supply with a fixed amount of heat, Qh.

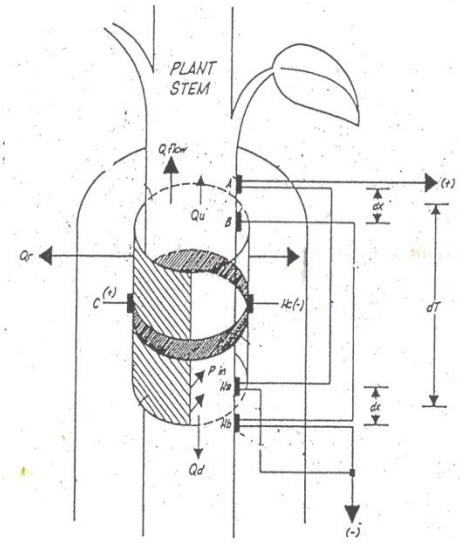

Figure 2.1: showing the schematic of Dynagauge for measuring Sap flow (adapted from Van Bavel ,1999)

Qh is equivalent to the power input to the stem from the heater, Pin, Qr is the radial heat conducted through the gauge to the ambient. Qv, is the vertical, or axial heat conduction through the stem and has two com[ponents, Qu and Qd. The heat convection carried by sap Qf, is determined by the measurement of Pin, Qu, Qd and Qr. Dividing the result by the specific heat of water and the sapflow temperature increase, the heat flux is converted directly to mass flow rate.

Energy Balance Equations

The energy balance is expressed as:

$$Pin = Qr + Qv + Qf$$

(2.35)

$$Pin = \frac{V^2}{R} \qquad (2.36)$$

(from ohm's law)

Fourier's law describes the vertical conduction components as:

Where Qv = Qu + Qd

$$Qu = KstA\frac{dTu}{dx}$$
$$Qd = KstA\frac{dTd}{dx} \qquad (2.37)$$

Where Kst is the thermal conductivity of the stem (W/m/K), A is the stem cross-sectional area (m^2), the temperature gradients are dTu/dx and dTd/dx (K/m), dx is the spacing between thermocouple junctions (m). One pair of the thermocouple is above the heater and one pair is below the heater as shown in Figure2.3

There are two differentially wired thermocouples both measuring the rise in sap temperature. Channel AH measures the difference in temperature A-Ha (mv). Channel Hb measures the difference in temperature B-Hb (mv). Subtraction of these two signals we obtain

BH-AH= (B-Hb)- (A-Ha)= (B-A) +(Ha-Hb) (mv) (2.38)

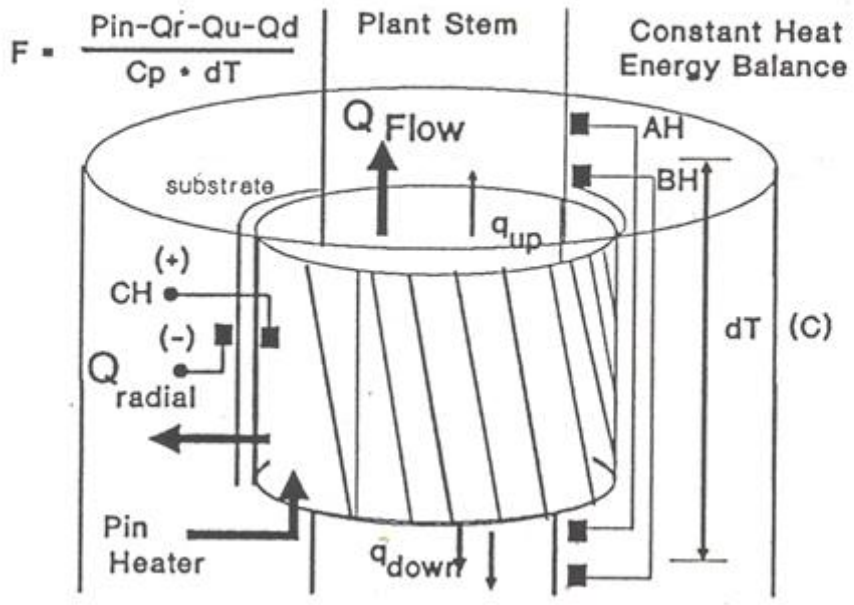

Figure 2.3: The diagram showing the connection of Dynagage for determination of transpiration (Van Bavel,1999)

The result gives the two components of axial heat conduction out of the stem section, Qu and Qd.

Since the distances, dx, separating the upper thermocouples pair and lower thermocouples pair are fixed by design for each particular gauge to the same value, the components of Qv are combined with a common denominator.

$$Qv = KstA\frac{BH - AH}{dx * 0.04mv/°C} \qquad (2.39)$$

The factor 0.04mv/^{o}C converts the thermocouple differential signals to degrees Celsius. Kst values are given for varying stem conductivity, 0.42 W/m/K (woody stem), 0.54(herbaceous) and 0.28 (hollow).

2.5.3 Sap flow Thermodynamics

After solving equation (1) for Qf, the flow rate per unit is calculated from equation for sap flow as described by Sakuratani (1981) and Baker- Van Bavel (1987). This equation takes the residual of the energy balance in watts, and converts it to a flow rate by dividing by the temperature increase of the sap and the heat capacity of water. Water is 99% of the sap content and it is safe to assume the heat capacity, cp is constant to all stems.

$$F = \frac{Pin - Qv - Qr}{Cp * dT}(g/s) \tag{2.40}$$

In equation (2.40) the radial heat loss is computed in as:

$$Qr = Ksh * CH \tag{2.41}$$

Ksh is the thermal conductance constant for particular gauge installation, Cp is the specific heat of water (4.186J/g*C), and dT is the temperature increase of the sap.

The Ksh is determined using conditions when sap flow is zero, substituting into equation (2.41) we obtain

$$Qr = Ksh(CH) = Pin - Qv \tag{2.42}$$

$$Ksh = \frac{Pin - Qv}{CH}(W/mV) \tag{2.43}$$

From measurements Ksh is obtained from zero flow, this is usually observed in pre dawn conditions between 0200hrs and 0400hrs.

The temperature increase of the sap, dT, is measured in mV by averaging the AH and BH signals, and then converted to degrees Celcius by dividing by the thermocouple temperature conversion constant as follows:

$$dT = \frac{(AH + BH)/2(mV)}{0.040mV/C} \tag{2.44}$$

Methodology

3.0 Experimental Sites and Location

The experiments were done in two phases in Harare, Zimbabwe at approximately 17,8^{o}S, 31.1E and at an altitude of approximately 1483m. The first phase was instruments calibration that was done at the University of Zimbabwe in the Agricultural Meteorology laboratory, Physics Department. The second phase where two automatic weather stations were installed to measure weather parameters for the determination of mass andenergy and transpiration of crops inside the greenhouse were done at Floraline (Pvt) Ltd, that is about 5km from the University of Zimbabwe.

3.1 Description of the site and greenhouse

All experiments were carried out in a 3-span commercial Azrom type greenhouse (Figure 3.1) at Floraline (Pvt) Ltd in Zimbabwe (17.8^{o}S, 31.1E, altitude 1500m) between September 2009 and April 2010. Each span of the greenhouse measured 9.6m wide and 44m long, with ridge and gutter heights of 6.5m and 4.1m, respectively. The ridges were oriented north- south, the greenhouse total floor area was 1267m^{2} and the roof sloped at about 26^{o} to the horizontal. The cladding material was 200µm polyethylene film with terrestrial infrared and UV absorbing additives (Ganeiger Co, Israel). The roof vents (one in each span on the west side of the roof) were located along the whole length of the ridge and were 1.4m, wide, with maximum opening angle of 34^{o} with the roof. The polyethylene side could be rolled up from the 2m above the floor to 3..35m on the south wall and to 3.45m on the north wall. The side and roof vents positions were controlled by an automated climate control system (NETAFIM NETAGROW Version 718.3 Priva, Israel) in response to ventilation temperatures (temperature at which ventilation begin) which are calculated on the basis of set ventilation temperatures and a number of influences, such as the measured inside air temperature and relative humidity and outside conditions.

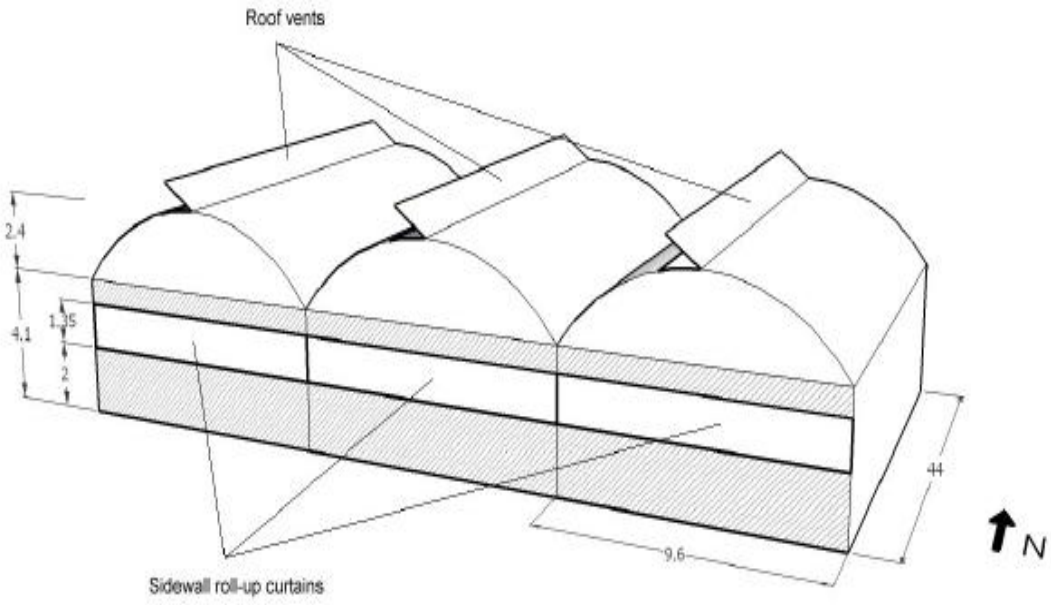

(a)

(b)

Figure 3.1: showing (a) a schematic representation showing dimensions of the greenhouse (b) the commercial greenhouse at FloralinePvt Ltd where the inside automatic weather station was installed

Two circulation fans, 0.75m in diameter with a rated outflow of 16 00m^3/hr at zero static pressure (blowing N-S) were installed under each gutter at a height 3.5m and 12m from the north and south wall respectively. The plants were planted in the greenhouse included several cultivars of roses, grown in

vermiculite medium in slightly raised 20mx0.45mx0.2m containers which were watered through an automated drip system. The total area of the vegetation cover represented about 40% of the total greenhouse floor. The containers were laid parallel to the gutters in twelve 20m rows in each span. The greenhouse roses were a variety of cultivars which included commercial ones line Nectarine, Betsy, King Arthur, Upendo and SymphonicaRosso.

3.2 Climatic and Physiological measurements

Climatic data were measured by two Automatic weather stations (AWS), one inside the greenhouse and other outside. The external station was sited in an open space, which was clear of buildings and obstacles. The external AWS provided climatic data of air temperatures and humidity, incoming solar radiation, wind speed and direction, PAR (Photosynthetically active radiation) and diffuse radiation. The atmospheric conditions inside the greenhouse were continuously monitored by the AWS included air temperature and relative humidity, net radiation, incoming solar radiation and PAR above the canopy, leaf temperature and soil temperature.

3.2.1 Climatic measurements outside the greenhouse

The external automatic weather station Figure 3.2 was installed at an open space which was free from obstacles and buildings and was used to measure the following weather parameters:

The outside ambient air temperature and relative humidity were measured at 1.5m above ground by means of temperature and humidity probe with serial number RHT 261 equipped with a capacitative relative humidity chip and a platinum resistance thermistor (model RH2nl,Delta T Devices, Cambridge,UK). The incoming solar radiation, PAR, wind speed and direction were measured at 2m above ground.

Figure 3.2: The external weather station at FloralinePvt Ltd

The solar radiation was measured by a pyranometer CM3 637 (model CM3, Kipp and Zonen, Delft, Netherlands). Wind speed was measured by a cup anemometer, with serial number 5525 (model A100L2, Delta T Devices, Cambridge,UK). The wind direction was measured by a wind vane serial number 7879 (model WD1, Delta T Devices, and Cambridge, UK). The diffuse radiation was measured using a pyranometer CM3 638 (model CM3, Kipp and Zonen, Delft, Netherlands) mounted on the shade ring. All outside measurements were automatically recorded on DL2e data logger (Delta T Devices, Cambridge, UK) every 5 seconds and averaged over 30minutes.

3.2.2 Climatic measurements inside the greenhouse

The internal automatic weather station (AWS), Figure 3.3, was installed approximately at the centre of the greenhouse. The climatic parameters which were measured by the AWS included temperature and relative humidity at above soil heights of 0.4 m and 0.8 m (within the canopy) and on top of the canopy at 1.5 m and 2 m (just below the roof of the greenhouse) in order to investigate possible vertical gradients of air temperature and relative humidity. To test the homogeneity within the greenhouse, the relative humidity and temperature were measured at the centre of the greenhouse and at four other positions at 1.5 m above soil surface (see Figure 3.4) by temperature humidity probes (model HMP45C, VaisalaInc,Boston,USA). The greenhouse internal air temperature and humidity were taken as the average of the five sensor positions. The net radiation, PAR, the incoming solar radiation were measured above the canopy and the soil temperature measured at two positions in the vermiculite medium. Leaf temperature was measured at six positions.

Figure 3.3: The Automatic weather station (AWS) inside the greenhouse at FloralinePvt Ltd.

The incoming solar radiation was measured with a tube solarimeter TSL29 (model TSL, Delta T Devices, Cambridge, UK). The net radiation was measured by the net radiometer equipped with coated Teflon coated sensor surfaces with serial number Q03194 (model Q7, Radiation and Energy Systems, Seattle, Washington, USA). The relative humidity and temperature were measured using the temperature humidity probes equipped with capacitive relative humidity chip and a platinum resistance thermistor (model RHT2nl, Delta T Devices, Cambridge, UK and HMP45C, Vaisala Inc., Boston, USA). The photo synthetically active radiation (400-70µm) was measured using a quantum sensor with serial number PAR 639 (model PAR-LITE, Kipp and Zonen, Delft, Netherlands).

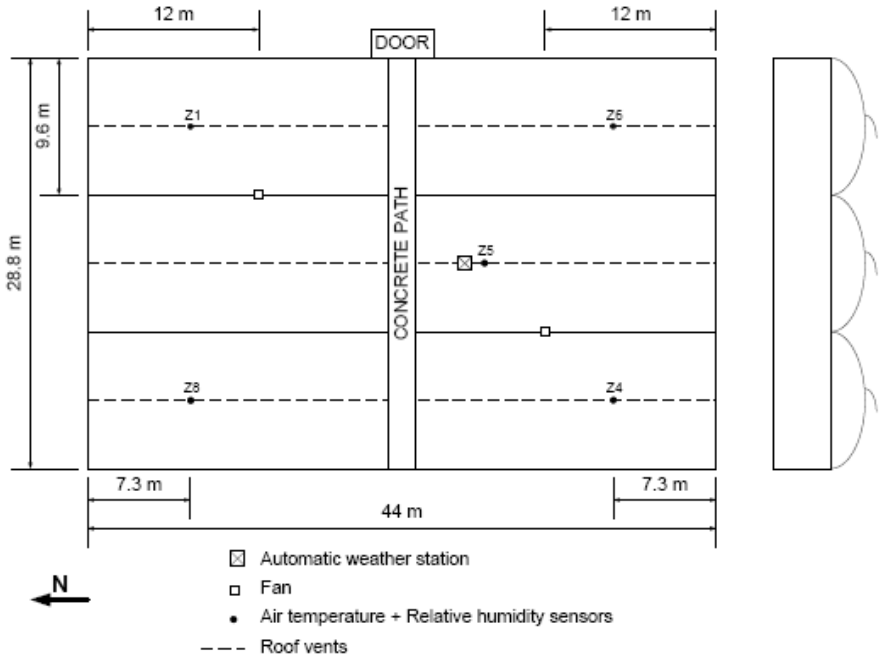

Figure 3.4: The positions of air temperature and relative humidity sensors within the greenhouse

The leaf temperature was measured at six positions with fine chromel-alumel thermocouples, type K, 0.2mm in diameter, attached to the lower side of leaf by paper clips.

The leaf temperature was taken as the average of six leaf temperatures. The vermiculite temperature at two positions were measured with by soil temperature probes (type STI, Delta T Devices, Cambridge, UK), and the average of the two readings was taken as vermiculite temperature.

All measurements were automatically recorded by the two data loggers, one that was Campbell Scientific data logger CR23X (Campbell Scientific Ltd, Shepshed, UK) that recorded measurements every 5second and averaged over , and DL2e data logger (Delta T Devices, Cambridge, UK) which recorded every 5seconds and averaged over 30minutes.

3.3.3 Leaf temperature sensors

Figure 3.5: The picture showing thermocouples attached to the underside of the leaf for measuring leaf temperature

Two types of leaf temperature sensors were used, leaf temperature thermocouples and radiation thermometer

3.3.3.1 Leaf temperature thermocouples

The thermocouples used were type K(chromel-alumel) with 200µm diameter. These were clipped onto the underside of the leaves by plastic paper clips as shown in Figure 3.5. The sensitivity curves for each type of thermocouple are pre-recorded in the data logger so that the thermocouple outputs were displayed in ^{o}C.

To check the reliability of thermocouples an infrared radiation thermometer was used on selected days. An infrared radiation thermometer utilizes the principle that: above absolute zero, all bodies emit electromagnetic radiation with wavelength and density which depends on temperature. The radiation emitted by a body also depends on its emissivity which is less than 1 for real bodies. The emissivity depends on the nature of the surface of the material, on the material itself and on the wavelength. If the emissivity is known, the temperature of the object can be determined by measuring the infrared radiation emitted by the object. Radiation thermometers are used to measure this kind of radiation, which includes a reflected component from the surrounding emitters. As the measurement is taken without the radiation thermometer contact with the object, so there no distortion of the temperature field. Most radiation thermometers allow for the emissivity setting on the sensor to be set to a correct value applicable to the surface to be measured.

3.3.5 Soil temperature probe

The soil temperature was measured using the soil temperature probe (type STI, Delta T Devices, Cambridge, UK). The thermistor is designed for measuring temperatures in the range -40ºC to 56 ºC. The major error component is the tolerance specification of the thermistor, which is ±0.32ºC from -20ºC to 60ºC.

4.0 Results and Discussions

Validation of Penman Monteith Method

The ventilation rate was determined using the water vapour balance method in equation (3.14); the transpiration term was evaluated using the Penman-Monteith method as was applied by (Katsoulas et al 2001). To validate the Penman Monteith method it was compared with Sap flow measurements using historical data (Mashonjowa et al 2007). Figure 4.1 shows the correlation between transpiration rates obtained from sap flow and determined by Penman Monteith formula using data from 1 December 2007-31 December 2007.

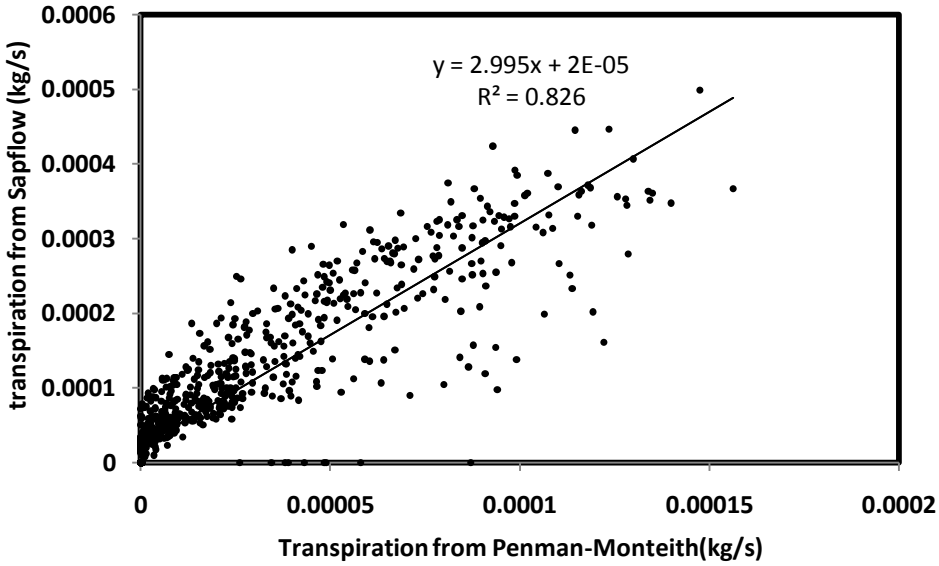

Figure 4.1: correlation between transpiration obtained from sap flow and transpiration obtained from Penman-Monteith method on days 1-31 December 2007

The results showed there is a good fit between the measured transpiration rates from sap flow gauges and the calculated transpiration rates from Penman-Monteith, although the sap flow gauges tends overestimate the crop transpiration in the morning (just after sunrise), and underestimate of crop transpiration in the afternoon (just before sunset) as reported by the following authors (Baker and van

Bavel, 1987; Baker and Nieber, 1989 and Grime et al (1995)). This was explained as follows, in the morning when soil temperature exceeds air temperature; there is negative temperature gradient in the sensor as warm sap enters a cooler stem, causing a temporary over-estimation of whole-plant transpiration, if the sensor is near the soil. In the afternoon, when the ambient air temperature is higher than soil temperature, the sensor registers a higher positive gradient in the sensor, resulting in an underestimation of whole plant transpiration. The errors can also be attributed to up scaling of the leaf transpiration that is based on the assumption the transpiration from the single is uniform throughout the whole canopy.

Determination of stomatal resistance

The version Penman-Monteith formula which was adopted for determining transpiration rates required the measurements and estimation of aerodynamic resistance and canopy stomatal resistance. The aerodynamic resistance for plants in a greenhouse was assumed to be 200sm^{-1}. The stomatal resistance in this study was obtained from the stomatal sub-model equation (3.22) in the GDGCM. Before use the stomatal model was calibrated to obtain the equation parameters by experimental data fitting into a statistical package Sigma plot. It was then validated by comparing measured stomatal resistance with predicted stomatal obtained from the model. The fig 4.2 shows the variation of solar radiation and stomatal resistance.

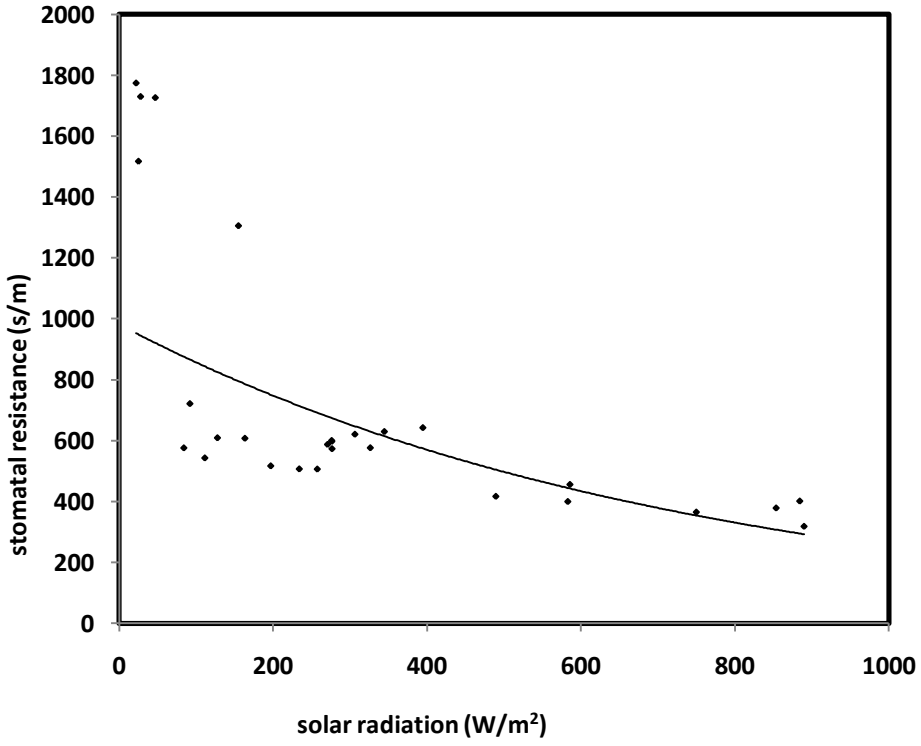

Figure 4.2: Variation of measured stomatal resistance and solar radiation on 28 February 2010 -14 March 2010

Figure 4.2 presents the variation of stomatal resistance and solar radiation. An increase in solar radiation results in a decrease in the stomatal resistance. Figure 4.2 can be used to explain why transpiration is high during the day and almost zero at night. During the day, transpiration is high because the incident solar radiation is high and the canopy stomatal resistance is low. During the night the stomatal resistance is much higher because solar radiation is zero and consequently transpiration is very small because the radiative component in equation (2.29) is almost equal to zero.

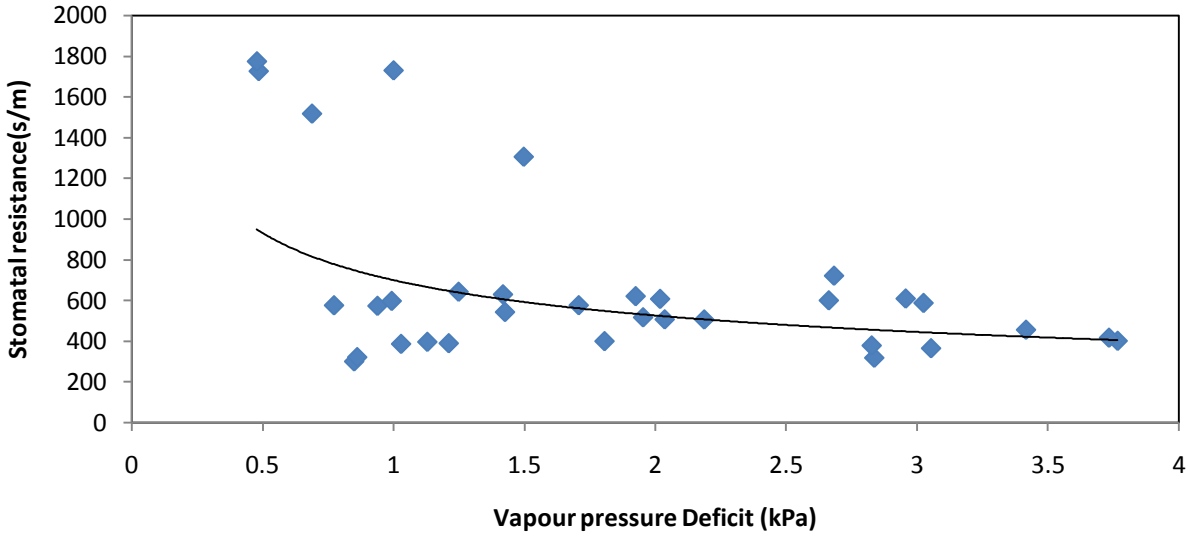

Figure 4.3: Variation of measured stomatal resistance with vapour pressure deficit (VPD) on 28 February 2010-14 March 2010

Figure 4.3presents the variation of measured stomatal resistance with vapour pressure deficit. It can be observed that high vapour pressure deficit corresponded to low stomatal resistance, and when the vapour pressure deficit was low, the stomatal was very large. This can be explained as follows: high vapour pressure deficit that occurs when temperature is high and because air can hold more vapour when its temperature rises. The vapour deficit between the leaf and the vapour pressure deficit becomes large and causes stomatal resistance to decrease rapidly . Low temperatures make the air more humid and it also tends to decrease the vapour pressure deficit that tends to increase the stomatal resistance.

Figure 4.3 shows variation of stomatal resistance and vapour pressure deficit (VPD) on 28 February 2010-14 March 2010. Figure 4.3 shows that as vapour pressure deficit increases, the stomatal resistance decreases, and a low vapour pressure deficit 0.48kPa corresponded to a high stomatal resistance of 1775s/m. Figure 4.8 shows peaks of the VPD corresponded to high stomatal resistance. The variation of measured stomatal resistance with vapour pressure deficit showed that low stomatal resistance is high solar irradiance, thus high vapour pressure deficit occurred when there was high solar irradiance which corresponded to high internal air temperatures and low internal relative humidity.

Table 4.1: Model specific parameters obtained in this study compared to those found by Baille et al (1994c) and Kittas et al (1999) for two cultivars of roses (Rosa x Hybrida)

	This study	Baille et al	Kittas et al
Cultivarand Substrate	Average of several cultivars in vermiculite	cv Sonia in rockwool	cv First Red in perlite
a	546.9752±93.1	349	566
b	52.3263±17.2	28	90
c	-0.1299±0.1	1.45	0.276

Table 4.1 shows the parameters of the stomatal model found by experimental data fitting using a statistical package Sigma plot and what has been found out by other authors; the values obtained in this study was comparable to what has been found out by Kittas et al (1999). However the was great difference to what has been found by Baille et al (1994c), this could be due to different locations , the growing medium of the roses and due to different cultivars. To test the reliability of the stomatal model it was validated by comparing predicted canopy stomatal resistance and measured stomatal resistance.

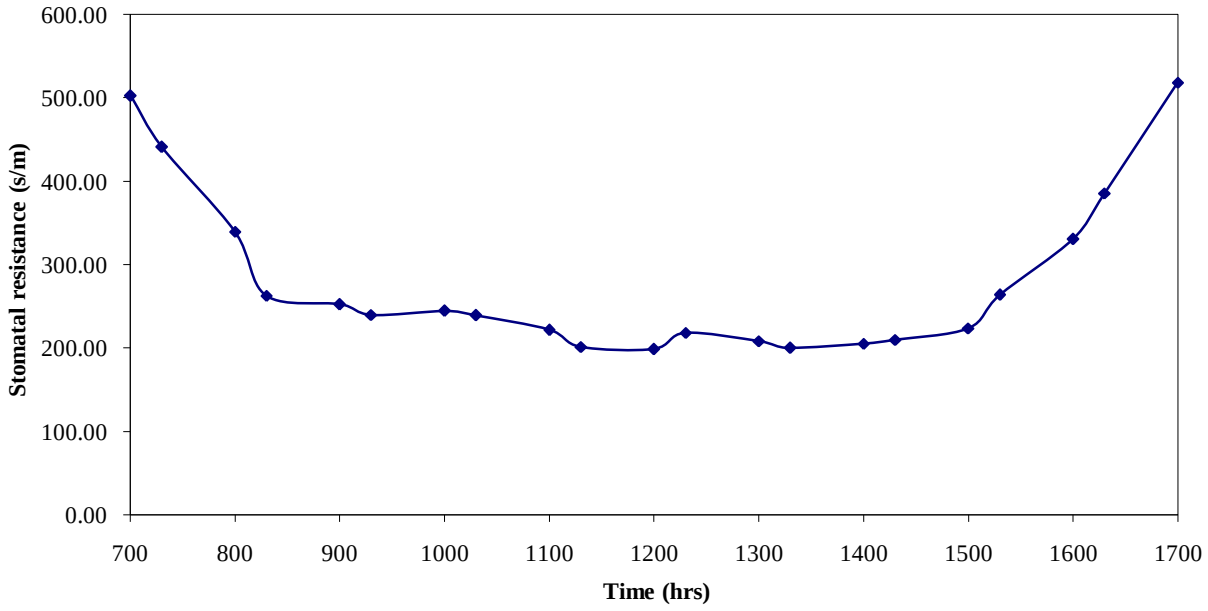

(a)

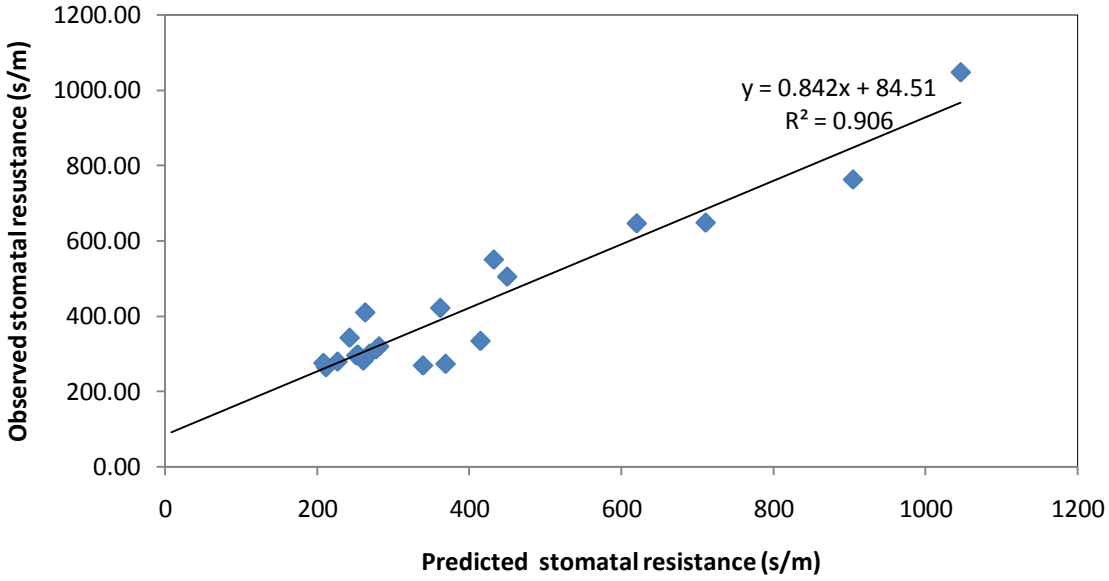

(b)

Figure 4.1: Showing (a) the daytime variation of stomatal resistance and (b) the correlation between observed stomatal resistance and predicted stomatal resistance on 16 March 2010

Figure 4.4 shows diurnal variation of stomatal resistance. Stomatal were high in the morning and late afternoon. During the day, the stomatal resistance was low and almost constant, and it was 200 sm^{-1}. There was an increase in stomatal resistance from 1500hrs to 1700hrs.

The Figure 4.4 (b) shows there was good fit between the measured canopy stomatal resistance and the simulated canopy stomatal resistance and therefore the stomatal resistance which was required in determination of the transpiration was estimated using the model equation (3.22).

Statistically analysis for stomatal model validation and calibration is shown in Table4.3. The t test was used to carry out the significance to test the null hypothesis H_0 that there is no significant difference between the observed stomatal resistance and predicted stomatal resistance. In both calibration and validation (Table4.1) we accepted H_0 since $|t_{Stat}| < t_{\alpha=0.025}$ and concluded that there was no significant difference between the modeled and the measured stomatal resistance at 5% level of significance

Conclusions and Recommendations

The results indicated that the greenhouse is greatly affeced by the mass and energy balance. It was concluded that the ventilation rate plays the pivotal role in driving the mass and energy balance in a greenhouse. The mass and energy balance influences the microclimate of a greenhouse and enables framers to grow crops in favourable conditions and ultimately improves the yield.

Referees

American Society of Heating, Refrigeration and Air-conditioning Engineers (ASHRAE) ,2005. ASHRAE Handbook of Fundamentals, **Chapter 27**: Ventilation and Infiltration. Atlanta, GA.

Baille, A., 1992. Thermique of Energetique des serres, Cours de Diplomed'Agronomie Approfondie, de Gẽnie Agronomique40, Montpellier, France, E.N.S.A.

Baille, A., Kittas, C. andKatsoulas, N., 2001. Influencing of whitening on greenhouse microclimate and crop energy portioning.

Bakker, J.C., Bot, G.P.A., Challa, H., N.J. van de Braak (Editors). 1995. Greenhouse Climate Control: An Integrated Approach. Wageningen, The Netherlands. WageningenPers Publisher.

Baptista, F.J., Bailey, B.J., Randall, J.M. and Meneses, J.F., 1998. Greenhouse Ventilation Rate: Theory and Measurement with Tracer Gas Techniques. Journal Agricultural Engineering Res (1999)**72,** pg363-374

Bartzanas, T., Katsoulas, N., Kittas, C., Boulard, T., Mermier, M., 2005.Effect of vent configuration and insect screen on greenhouse microclimate.International Conference "Passive and Low Energy Cooling for the Built Environment", Santorini, Greece.

Bot, G.P.A., 1983.Greenhouse Climate from physical processes to a dynamic model.Ph.D. Thesis, University of Wageningen, Wageningen, The Netherlands.

Boulard, T., 1993.Experimental and modeling study on greenhouse natural ventilation; recapitulative of the 1988-1992 experiments.Note interne I.N.R.A. **93-1**, Station de ^Bioclimatologie de Montfavet, France.

Boulard, T., Baille, A., 1995. Modeling of air exchange rate in a greenhouse equipped with continuous roof vents. Journal Agricultural Engineering, Research **61**, pg 37-48.

Boulard, T., Wang, S. 2000. Greenhouse crop transpiration simulation from external climate conditions.Agricultural and Forestry Meteorology **100**, pg25-34.

Bruce, J.M., 1982. Ventilation of a model livestock building by thermal buoyancy.Transactions of the ASAE, **25161,** pg1724-1726.

Chou, S.K., Chua*, K.J., Ho, J.C., Ooi, C.L., 2004.On the study of an energy-efficient greenhouse for heating, cooling and humidification applications. Applied Energy 77, pg 355-373

De Jong, T., 1990.Natural ventilation of large multi-span greenhouses. Ph.D. Thesis, University of Wageningen, Wageningen, The Netherlands.

Demrati, H., Boulard, T., Bekkaoui, A. and Bouirden, L., 2001.Natural ventilation and microclimatic performance of a large-scale banana greenhouse.J.agric.Engng Res.,**80(3)**: 261-271

Demrati, H., Boulard, T., Bekkaoui, A., Fatnassi, H., Majdoubi, H., Elattir and

Dynamax Inc. (2005) DynagageSapflow sensor user manual.Dynamax Inc., 10808 Fallstone Rd. Houston TX77099, USA (http://www.dynamax.com)

Fatnassi, H., Boulard, T. and Bouirden, L., 2003. Simulation of climatic conditions in full-scale greenhouse fitted with insect-proof screens. Agric. For.Meteorol., **118**: 97-111

Fatnassi, H., Boulard,T., Demrati, H., Bouirden, L., Seppe, G., 2001. Ventilation Performance of a large Canarian-Type Greenhouse equipped with insect- proof nets. Biosystems Engineering, **82(1),** 97-105.

Fernandez, J.E., Bailey, B.J., 1992. Measurement and Prediction of greenhouse ventilation rates. Agricultural and Forestry **58**, pg229-245.

Fuchs, M., Dayan, E., Shmuel, D., Zipori,I., 1997. Effects of ventilation on the energy balance of a greenhouse with bare soil. Agricultural and Forestry Meteorology **(86).,** 273-282.

Fuchs, M., Segal. Dayan, E., Jordan, K., 1996. Improving greenhouse microclimate control with help of plant temperature measurements. BARD project No IS- 1816-90R. Final report 2.

Gandemer, J. and Bietry, J.1989, Coursd'aërodynamique.REEF, **vol2**, Sciences du Batiment - CTBS Nantes

Hanan, J.J., 1998. Greenhouses: Advanced technology for protected horticulture. CRC Press. London. 684pp

Harmanto, Tantau, H.J and Salonke, V.M., 2006. Microclimate and air exchange rates in greenhouses covered with different nets in the humid tropics. Biosystems Engineering, **94(2):** 239-253

Jarvis, P.G., 1985. Coupling of transpiration to the atmosphere of horticultural crops.Acta Horticulturae**.171**: 187-205

Jones, H.G., 1992. Plants and microclimate. Cambridge University Press, UK

Katsoulas, N., Bartzanas, T., Boulard, T., Mermier, M. and Kittas, C., 2006.Effect of vent openings and insect screens on greenhouse ventilation.Biosystems Engineering, **93(4):** 427 – 436

Kittas, C. Katsoulas, N., and Baille, A., 1999. Transpiration and Canopy Resistance of Greenhouse Soilless Roses: Measurements and Modelling. Acta. Hort. **507**:61-68

Kittas, C., Boulard, T. and Papadakis, G., 1997. Natural ventilation of a greenhouse with ridge and side openings: Sensitivity to temperature and wind effects. Transactions of the ASAE, **45(4)**: 415-425

Klein,S.A., Beckham, W.A., Cooper, P.I., Dufie, N.A., Freeman, T.L., Mitchel, J.C., Beekman, D.M., Oonk, R.L.,Hughes, P.J., Eberlein, M.E.,Karman, V.D., Pawelski, M.J., Utzinger,D.M., Duffie, J.A., Brandemuehl, M.J., Arny, M.D., Theilacker, J.C., Morrison, G.L., Clark, D.A., Braun, J.E., Evans, B.L.& J.P. Kummer.1988. TRNSYS: A transient system simulation program. Engineering experiment station report **38-12**, Solar Energy Laboratory, University of Wisconsin-Madison, USA.

Mashonjowa, E., Ronse F., Milford, J.R, Lemeur, R., J.G., 2010b. Measurement and simulation of the ventilation rates in a naturally greenhouse in Zimbabwe. Applied Engineering in Agriculture, in press

Mashonjowa, E., Ronse, F., Milford, J.R., Lemeur,R., Pieters,J.G., 2010a. Calibration and validation of a dynamic model in Zimbabwe. Submitted to Agricultural and Forestry Meteorology

Mashonjowa, E., Ronse, F., Pieters, J.G., Lemeur, R., 2007b.Modelling heat and mass transfer in naturally ventilated greenhouse in Zimbabwe. Applied Engineering in Agriculture, in press

Monteith, J.L., 1973. Principles of Environmental Physics, Arnold, Paris

Monteith, J.L., Unsworth. 1990 Principles of Environmental Physics, Edward and Arnold, UK

Papadakis, G., Frangoudakis, A. and Kyritsis, S., 1994.Experimental investigation and modeling of heat and mass transfer between a tomato crop and the greenhouse environment. J. Agriculture Engineering. Res., **57**: 217-227

Pasian, C.C. and Lieth, J.H., 1989. Analysis of response of net photosynthesis of rose leaves of varying ages to photosynthetic active radiation and temperature. Journal American Society Horticulture Science **114(4):** 581-586

Pieters, J.G., and Deltour, J.M., 1997. Performances of greenhouses with the presence of condensation on cladding materials.J.Agriculture Engineering. Res., **68(2),** 125-137.

Rosenberg, N.J., Blad, B.L. and Verma, S.B., 1983. Microclimate: Biological environment. Second Edition. John Wiley &Sons, New York

Roy, J.C., Boulard, T., Kittas, C. and Wang, S., 2002. Convective and ventilation transfers in greenhouses, part 1: the greenhouse considered as a perfectly stirred tank.

Biosystems Engineering, **83(1):** 1 - 20

Seginer, L., 1984.Transpirational cooling of a greenhouse crop with partial ground cover. Agricultural and Forestry Meteorology **100**, pg 265-281.

Stanghellini, C., 1987. Transpiration of greenhouse crops; An aid to climate management. Ph.D. Thesis, University of Wageningen, Wageningen, The Netherlands.